Investigating the role of target size and rigidity in phagosomal processing during phagocytosis

Author: Nathan Joyet (1404644), Master of Biotechnology specialization in medical biotechnology

Supervisors: Daan Vorselen, Youri Peeters

Place: Wageningen University and Research, CBI laboratory

Period: February - July

Abstract

Phagocytosis is a key immune process in which professional phagocytes, such as macrophages, engulf and break down pathogens, dead cells, and debris. This process is vital for maintaining tissue health. Modulating phagocyte function is also essential in various therapeutic strategies, including cancer immunotherapy. While we understand the molecular regulation of phagosomal maturation relatively well, we know much less about how the physical properties of the targets, especially shape, size and stiffness, affect this process. Although previous studies showed that the shape and stiffness of particles can influence uptake, the impact on what happens inside the cell is still mostly unknown [1–3]. A key question is how the rigidity of the cargo influences subsequent steps in phagosomal maturation, particularly for elongated particles where mechanical factors may alter their transport. In this study, we demonstrate that the rigidity and size of microrods interact in non-additive ways, impacting both uptake and phagosomal maturation. Using smaller microrods with varying stiffness (20 to 1000 kPa), we found a similar rigidity-dependent pattern of phagocytic uptake compared to longer (25 μm) microrods, suggesting that rigidity and size affect not just the engulfment but also the maturation of the cargo. Additionally, the buildup of actin at the ends of stiff, long microrods pointed to a mechanical disturbance in how the cytoskeleton reorganises and how lysosomes fuse with phagosomes. Here, we developed a ratiometric pH assay (FITC/Cy5) and confirmed that long, stiff rods had trouble with acidification, while smaller rods acidified well regardless of their stiffness. These findings reveal a mechanosensitive checkpoint in phagocytosis where the interdependent relationship between rigidity and size dictates the efficiency of phagosomal maturation.

Introduction

Professional phagocytes, such as neutrophils, dendritic cells and macrophages, play a crucial role in maintaining homeostasis within multicellular organisms through the clearance of bacteria, dead cells, and cellular debris via phagocytosis[4]. Due to its central role in immunity, there is growing interest in understanding the mechanisms that regulate phagocytosis, particularly in the context of developing novel immunotherapies for infectious diseases and cancer[5–8]. Phagocytosis proceeds through three stages, each of which can be disrupted in phagocytosis-related diseases. Initially, phagocytes recognise biochemical molecules on the surface of the encountered cargo, including opsonisation molecules (antibody, complement), PAMPS (Pathogen-Associated Molecular Patterns), or other cellular stress signals (lipopolysaccharide). This recognition is mediated by specialised phagocytic receptors for each ligand class, such as Fc receptors for antibodies and TLR4 for lipopolysaccharide[9,10]. Subsequently, Receptor engagement triggers a complete reorganisation of filamentous actin at the phagocytic interface, shaping the overlying plasma membrane into a phagocytic cup that engulfs the cargo. The engulfed cargo is ultimately enclosed within a maturing phagosome, which undergoes further processing to degrade the ingested material[11,12].

Phagosomal maturation is actively regulated by cytoskeleton proteins that relocate the cargo. During relocalisation, sequential acquisition of endosomal and lysosomal proteins occurs via fusion and fission events that progressively acidify the cargo, ultimately leading to the formation

of the phagolysosome [13] where degradation of the phagosomal content occurs [14–16]. Proteins central to this process are Rab GTPases, tethering factors, and SNAREs, which coordinate the trafficking and membrane fusion[17]. Additionally, the transport of phagosomes along cytoskeletal proteins plays a crucial role in coordinating the timing of biochemical events necessary for effective pathogen degradation, such as the transition from actin to microtubule. This transition functions as a "maturation clock", ensuring the timely acquisition of degradative capacity [16].

While phagocytosis is well studied from a molecular standpoint, emerging evidence underscores the critical role of cargo biophysical properties in regulating both uptake and subsequent maturation. To address some of these complexities, researchers have utilised artificial particles to mimic cellular properties. For example, DAAM particles (deformable poly-Aam-co-AAc microparticles) are a valuable tool for simulating the biophysical properties of living cells, particularly their stiffness[3]. By varying the composition of these particles, it is possible to produce particles with different sizes and stiffness, allowing for the investigation of how these properties affect immune cell-target interactions. This way, it has been shown that, during engulfment, the phagocyte exerts pressure to retract and encircle the target and applies significant constrictive pressures on its target during engulfment, which is highly affected by target characteristics like size and stiffness[1–3].

Beyond uptake, biophysical features of the cargo can also impact downstream phagosomal maturation. Notably, shape and size have been linked to delays or stalls in maturation. Recent studies have demonstrated that elongated particles can induce sustained actin polymerisation, leading to stalled maturation[18–20]. In contrast, while target stiffness has been established to affect phagocytic uptake [21], its influence on phagosomal maturation remains poorly understood. This represents a significant knowledge gap, particularly given the diversity of mechanical properties among cargos, ranging from rigid bacterial cell walls to deformable apoptotic cell bodies.

While these experiments clearly illustrate the functional role of mechanical properties in phagocytosis, they do not consider the combined effects of size, rigidity, and shape, which may lead to varying outcomes. For instance, while it's known that elongated shapes are engulfed less efficiently than spherical particles[22], and the phagosomal processing of these shapes can be highly affected, the role of stiffness on the uptake and phagosomal processing of elongated particles is still largely unknown[1].

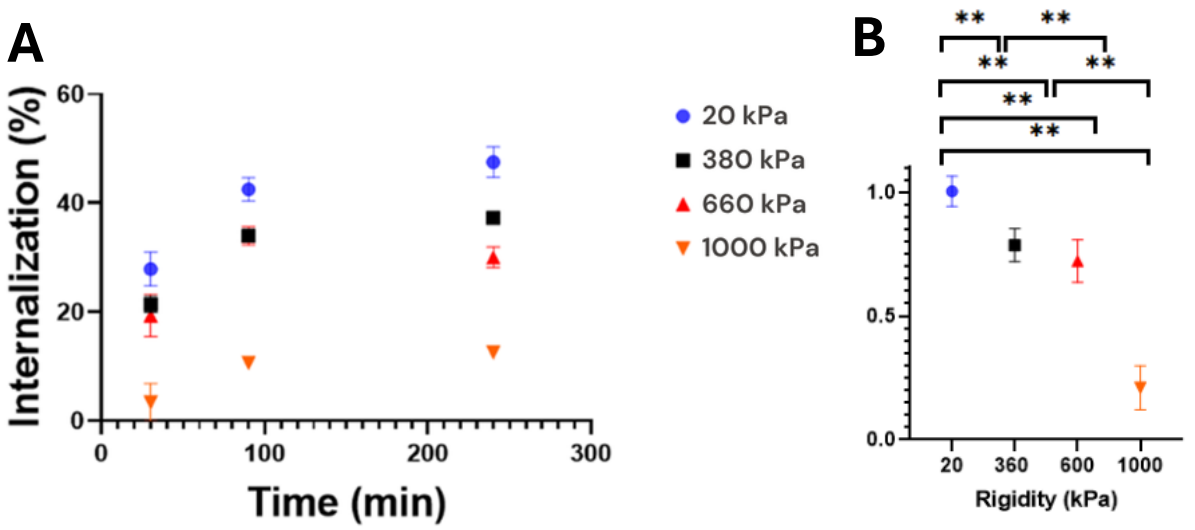

Figure 1: (A) Internalisation percentage of microrods of different rigidity (20, 380, 660, and 1000 kPa) by J774A.1 macrophages after 30, 60, and 120 min. (B) Internalisation efficiency values were normalised to the 20 kPa microrods. Stars indicate statistical ratio paired samples t-test significance, with two stars (**) for $p < 0.01$.

Therefore, efforts have been made to investigate the interplay between size and rigidity on the uptake by macrophages via the utilisation of microrods (2.5 × 2.5 × 25 µm) with varying rigidity. Indeed, macrophages showed a distinct rigidity-dependent uptake pattern when incubated with microrods, where softer, more flexible rods are taken up more efficiently than rigid ones (Figure 1). This increased uptake is hypothesised to be related to the flexibility of the particles, with bending of the rods occurring predominantly after internalisation (Figure 2). Additionally, preliminary data do not conclusively demonstrate that the observed differences in uptake are solely attributable to engulfment. Significantly, this raises the possibility that microrod stiffness may not only affect uptake, but also downstream intracellular processing, such as phagosomal maturation and lysosomal fusion. Since these processes are accompanied by progressive acidification of the phagosome, measuring the pH provides a crucial readout to assess whether and how microrod stiffness impacts phagosomal maturation. A delay or inhibition in acidification could indicate impaired fusion with lysosomes or altered trafficking, providing insight into the broader consequences of particle rigidity on macrophage function.

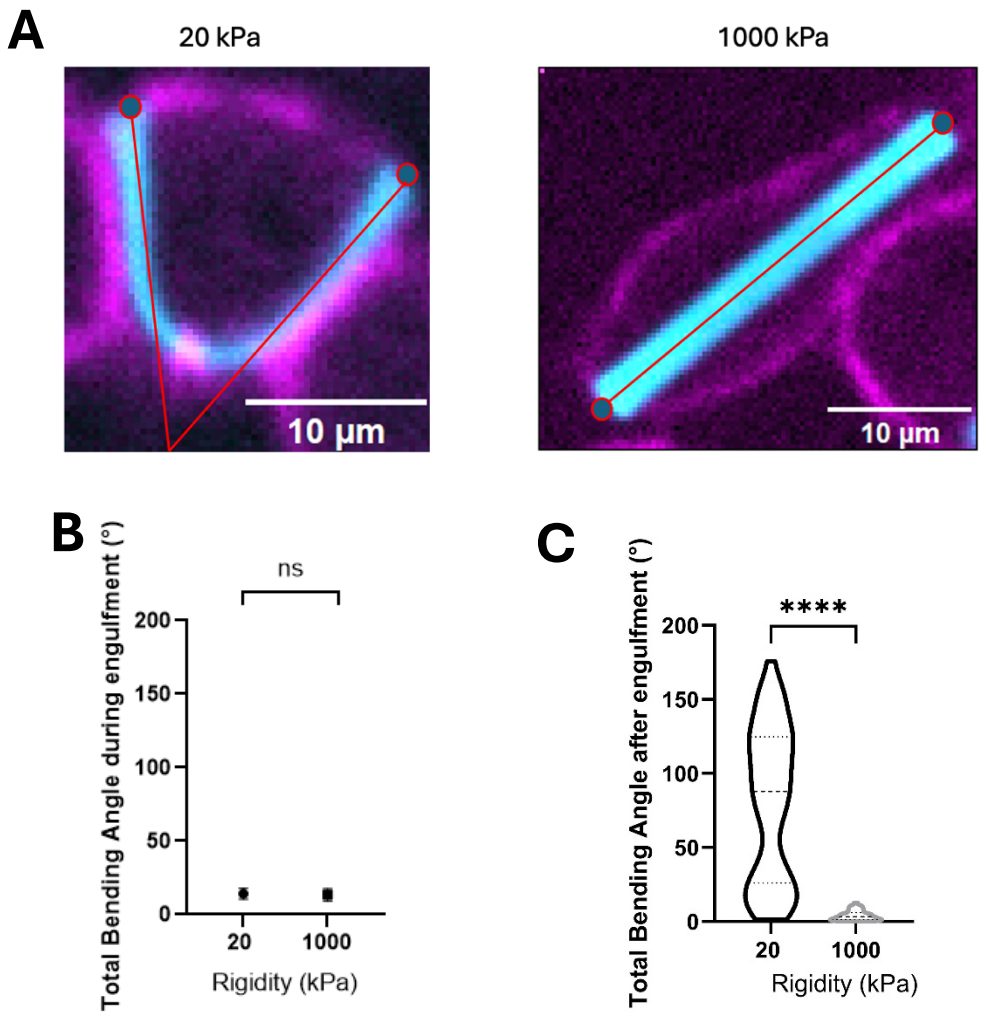

Figure 2: (A) Effect of substrate stiffness on macrophage morphology.
(F-Actin: Pink, Microrod: Blue.) (B and C) Degree of bending of internalised rods of different rigidity (20, 360, 600 and 1000 kPa) during engulfment (B) or after engulfment (C).
Data from Youri Peeters

Here, we investigated the fundamental mechanisms underlying the interaction between size and rigidity on phagosomal processing. Given that large cargo and continuous actin polymerisation have been shown to influence the specific steps of phagosomal maturation, we used smaller microrods with adaptable rigidity to investigate how rigidity impacts phagosomal uptake and subsequent processing. Experiments will be designed to quantify the differences in uptake between stiff and soft microrods, and to determine the extent to which rigidity impacts this process. We also developed a methodology that measures the stage at which cargo uptake is impaired by correlating the pH of the particle inside the cell with specific stages of phagosomal processing. This way, we will investigate how stiffness may affect other processes like phagosomal maturation and lysosomal fusion, beyond initial uptake.

Material and methods

Microrod Functionalization

Microrods were already available for this study throughout this manuscript. Microrods are further categorised by their size (small or big) and relative rigidity (soft, intermediate, or stiff). Specifically, 20 kPa as ‘soft’, 360 kPa rods as 'intermediate', and 600 kPa as 'stiff', with further distinction made where necessary based on their precise stiffness value and size.

Microrods were functionalized following a modified protocol[23]. Microrods were stored in MilliQ water. The rods were incubated with 20 mg/mL Bovine Serum Albumin (BSA) (Roche, Cat. No. 10735086001) for 72 hours at room temperature to facilitate diffusion and binding of BSA to the microgels via amine-GMA coupling. Subsequently, fluorophores (FITC-cadaverine and Cy5-cadaverine) (Invitrogen, Cat. No. A1318) were added to the rod-containing tubes at a final concentration of 0.2 mM and incubated for 2 hours. To block remaining glycidyl groups, 0.5x the original volume of blocking buffer (300 mM Tris (Invitrogen, Cat. No. 15504020) pH 9.0, 300 mM NaCl (Merck, Cat. No. 106404), 300 mM ethanolamine (Sigma-Aldrich, Cat. No. E9508)) and incubated for 2 hours at room temperature using a rotating stirrer. If rods were not used immediately, 10% w/v sodium azide (Merck, Cas. No. 822335) was added. The rods were then washed three times with 1x PBS pH 7.4 containing 0.1% Tween 20 (Sigma-Aldrich, Cat. No. 822184) and stored at 4°C until further use. Anti-BSA (MP Biomedicals, 0865111; RRID: AB_2335061) was added at a concentration of 0.1 mg/mL and incubated for 1 hour. Following this, rods were washed three times with 1x PBS pH 7.4 containing 0.1% Tween 20, with the final wash performed using 1x PBS pH 7.4. After the last wash, the rods were resuspended in 50 µL and stored at 4°C until further use. The number of rods was determined by counting with a hemacytometer. Centrifugation speeds and times for different rigidity microrods were applied as follows: 7000g for 10 minutes for 20 kPa and 360 kPa rods (10% and 20% wt monomer, respectively), and 2000g for 4 minutes for 1000 kPa rods (80% wt monomer).

pH-dependent fluorescence analysis of functionalized rods

Four different solutions were prepared: three PBS solutions ranging from pH 4 to pH 7.4, and one MES (Acros organics, Cat. No. 397351000) solution at pH 6. For each well, 30,000 rods were taken from the stock. The rods were washed once with the respective incubation solution using the same centrifugation speed and time as during functionalization. After washing, the rods were transferred to a 96-well plate in the pH buffer, ensuring a final volume of 300 µL per well. Each sample was then measured using the flow cytometer. FITC fluorescence intensity is pH-sensitive, and the fluorescence of FITC is quenched under low pH conditions. The raw data from the cytometer, including FITC and Cy5 intensity measurements, were analysed using FlowJo (v10) software. The ratio of FITC to Cy5 intensity was calculated for each sample. These ratios were then normalised to the values obtained from the PBS pH 7.4 measurements.

Cell Culture

J774s (or RAW 264.7s) phagocytic cells were maintained in complete DMEM medium, consisting of DMEM (Gibco, Cat. No. 42430-025) supplemented with 10% heat-inactivated Fetal Bovine Serum (FBS) (ThermoFisher, Cat. No. 10270106) and 1x antibiotics-antimycotics (AbAm) (ThermoFisher, Cat No. 15240-062). Cells were routinely split every 2-3 days (e.g., Monday, Wednesday, Friday) at a 1:6 ratio, or 1:8 on Fridays. For routine splitting, a new T75 flask was prepared with 12.5 mL of fresh complete DMEM medium. Cells were gently scraped from the surface of the old flask, and 2.5 mL of the cell suspension was transferred to the new flask.

Phagocytic Assay

For phagocytosis experiments, J774s phagocytic cells were seeded in 96-well plates at a density of 3.0×10^4 cells per well in 100 µL of complete DMEM medium (DMEM supplemented with 10% FBS and antibiotics/antimycotics). Cells were allowed to adhere overnight.

On the day of the assay, 1.8×10^5 functionalized microrods were prepared in 100 µL of complete DMEM medium. The existing medium in each well containing the cells was replaced with the microrod-containing solution. The plates were then centrifuged for 1 minute at 300 g to synchronise contact between cells and microrods. Following centrifugation, the plates were incubated at 37°C for the desired uptake efficiency experiment incubation time.

For flow cytometry analysis, cell strainer tubes were prepared with 200 µL of ice-cold PBS for each time point and condition. Then, they were placed in a bucket with ice. At the predetermined time points, the wells were scraped, and 100 µL of each cell suspension was transferred to the ice-cold PBS-containing cell strainer tubes. Samples were then directly measured on the flow cytometer. This process was repeated for all subsequent time points.

Microscopy Assay

J774s phagocytic cells were seeded in 96-well glass bottom plates (Cellvis, P96–1.5H-N) at a density of 3.0×10^4 cells per well in 100 µL of complete DMEM medium (DMEM supplemented with 10% FBS and antibiotics/antimycotics). Cells were allowed to adhere overnight at 37°C (Sheldon manufacturing inc., SCO5W).

On the day of the experiment, functionalized microparticles were counted using a hemocytometer. Microparticle solutions were prepared in fresh DMEM media at concentrations of approximately 1×10^5 rods in 100 µL.

Optional: For fixed cell staining, permeabilisation was performed before inside/outside staining. Cells were permeabilised by adding 0.2% Triton X-100 (Merck, Cat. No. 108603) in PBS to each well (1 mL per well for 12-well plates, 0.5 mL per well for 24-well plates). Cells were incubated for 10 minutes, followed by three rinses with PBS pH 7.4. Phalloidin (ThermoFisher, Cat. No. A12379) staining was performed using a working concentration of 0.15 µM, diluted 400x from the stock solution (66 µM in 30 µL DMF) in PBS. The PBS in wells was replaced with the phalloidin

solution, and cells were incubated for 30 minutes. After incubation, cells were rinsed three times with PBS.

The existing medium in each well was replaced with fresh DMEM medium containing the microparticles. Plates were then centrifuged at 300 g for 1 minute (Eppendorf, 5920R). Depending on the experiment, cells were either incubated at 37°C or directly imaged for live cell experiments. When varying incubation times with beads, microparticles were added at staggered times, and cells were fixed simultaneously.

Images were taken with a Leica SP8 confocal microscope. We used Z-stack imaging to confirm the uptake of microrods. We measured signal intensity with ImageJ. To do so, a line selection (e.g., straight, segmented, or freehand) is drawn precisely across the region of interest using the appropriate tool within ImageJ. Then, using the Analyse> Plot Profile menu command, the "Plot Profile" function is called. The “List” button generates a tabular representation of the plot; this raw data can then be copied for subsequent analysis.

Results

Small microrods exhibit a similar rigidity-dependent pattern of cargo clearance as larger microrods

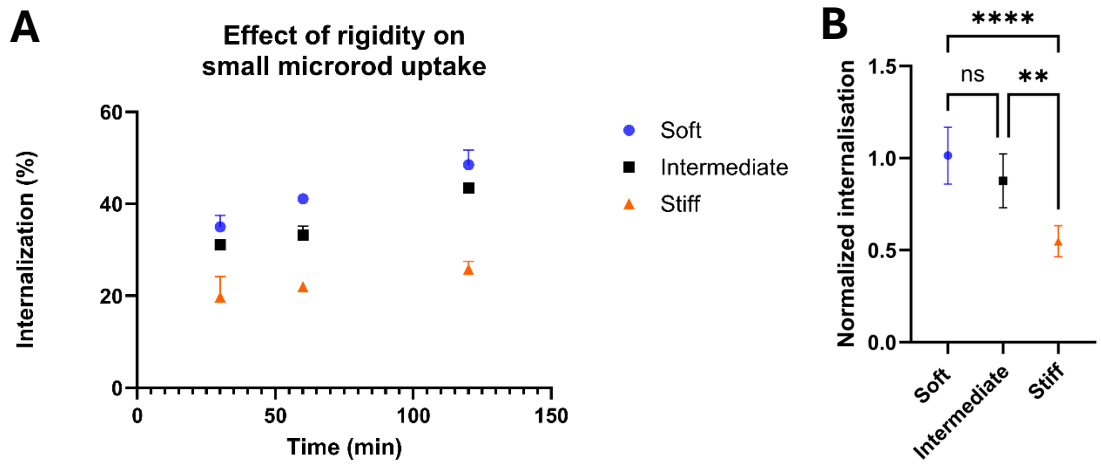

Figure 4: (A) Internalisation percentage of microrods of different rigidity (20, 360, and 1000 kPa) by J774A.1 macrophages after 30, 60, and 120 min. (B) Internalisation efficiency values were normalised to the 20 kPa microrods. Stars indicate statistical independent samples t-test significance, with two stars (**) for $p < 0.01$ and four stars (****) for $p < 0.0001$.

To investigate how the interplay between microrod size and rigidity affects phagocytic uptake, we incubated J774A.1 macrophages with small microrods (2.5 × 2.5 × 12.5 µm; L × W × H) of varying stiffness (20–1000 kPa). Internalisation was quantified by flow cytometry using the pH-sensitivity of FITC, which enabled discrimination between surface-bound and internalised microrods (Supplementary Figure 9). A clear stiffness-dependent uptake pattern was observed for the small microrods (Figure 4A), with the softest (20 kPa) microrods showing the highest internalisation

efficiency, reaching 47% after 120 minutes. In contrast, the stiffest microrods (1000 kPa) were internalised significantly less, with uptake reaching only 23% at the same time point. These results resemble those observed for long microrods, where internalisation reached 43% for 20 kPa rods and 16% for 1000 kPa rods after 120 minutes (Figure 1). Overall, smaller microrods were more readily internalised than the longest ones. These combined findings indicate that both microrod size and stiffness significantly influence macrophage phagocytosis, with a higher internalisation percentage for softer and smaller microrods.

Microrod rigidity dictates post-internalisation fate, especially for larger particles.

To explore how the impact of rigidity extends beyond initial uptake, macrophages were incubated with small microrods (12.5 µm) of varying stiffness (20–1000 kPa), followed by microscopic observations to track their intracellular location and state.

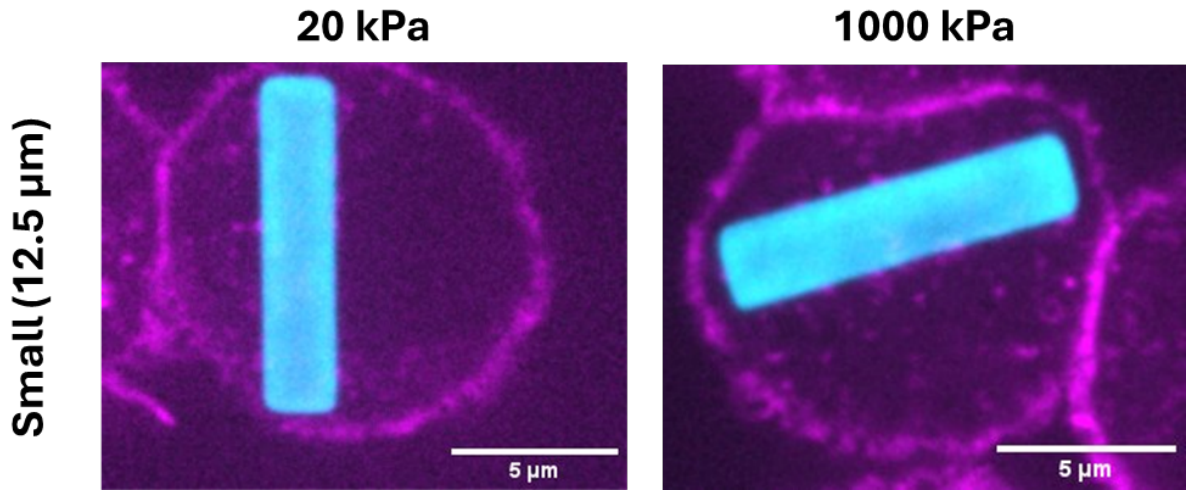

Figure 5: Effect of substrate stiffness on macrophage morphology. (F-Actin: Pink, Microrod: Blue.)

Distinct behaviours were observed based on microrod size and stiffness. Long, stiff microrods (25 µm, 1000 kPa) showed actin accumulation at their ends. This suggests impaired phagosomal maturation. In contrast, small microrods (12.5 µm) displayed different behaviours. The rigidity-dependent behaviours, such as actin accumulation at the poles and changes in rod straightness after internalisation, were not seen in the small microrods. These smaller rods remained straight and did not cause actin recruitment at their poles, regardless of stiffness.

Additionally, long soft microrods (20 kPa) were internalised. This indicates that flexibility plays a role in cargo elimination rather than cellular uptake. These findings suggest that rigidity affects not only the initial internalisation efficiency but also the processing after internalisation. This is particularly true for larger constructs, as it influences later events like phagosomal maturation and the physical shape of the internalised cargo within the cell.

FITC/Cy5 ratio enables reliable pH quantification across microrod types

Given the general reduced uptake of stiff microrods and preliminary indications of reduced acidification in long, stiff microrods, we aimed to quantify the intracellular pH following microrod uptake. We established a ratiometric fluorescence approach based on the pH-sensitivity of FITC. Since internalised microrods displayed fluorescence changes consistent with acidification, we hypothesised that the FITC/Cy5 ratio could be used to track phagosomal pH dynamics and identify the potential compromised phagosomal step following microrod uptake.

To generate calibration curves, functionalized microrods of varying size (small: 12.5 µm; big: 25 µm) and rigidities (360 and 1000 kPa) were incubated in PBS adjusted to pH 4, 6, and 7.4. These pH values were chosen to represent the physiological range during phagosomal maturation. This range goes from the relatively neutral extracellular environment at pH 7.4 to the more acidic conditions found in maturing phagosomes, reaching as low as pH 4. As anticipated, the FITC fluorescence signal demonstrated an explicit pH dependency, with fluorescence intensity decreasing significantly as the pH becomes more acidic (Figure 6).

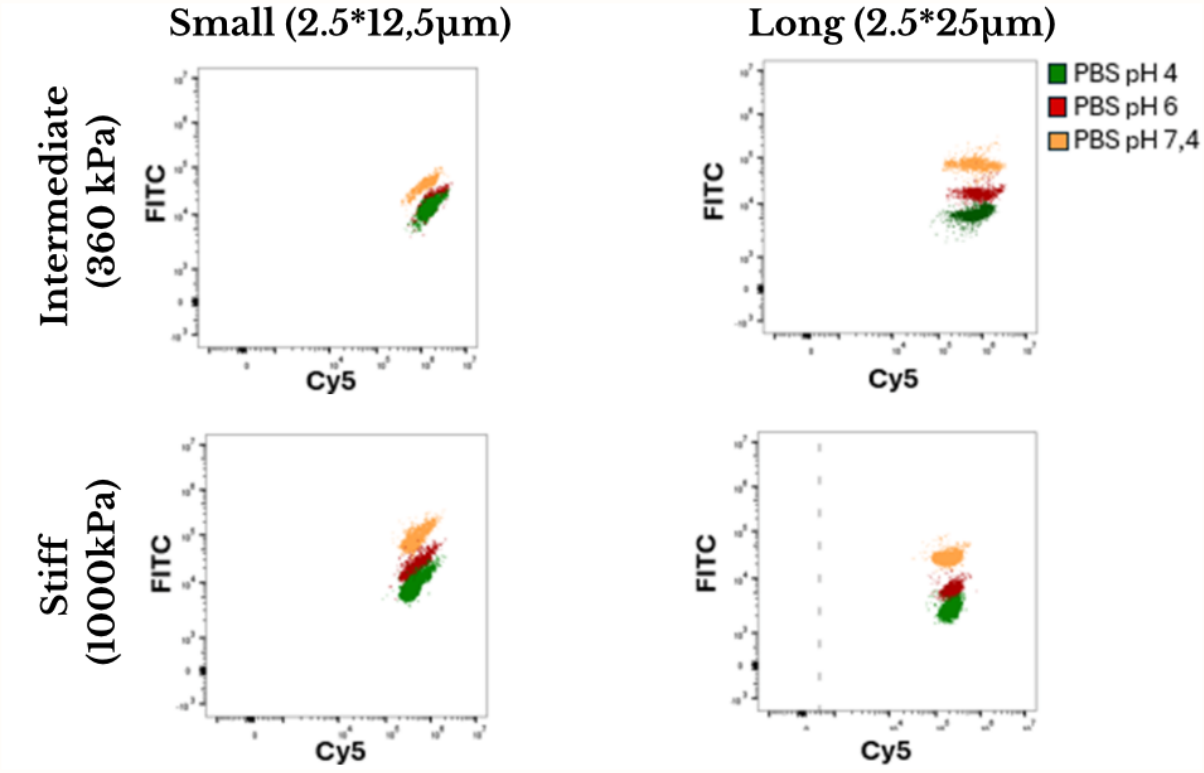

Figure 6: Representative flow cytometry dot plots of small (2.5 x 12.5 µm) and long (2.5 x 25 µm) microrods with intermediate (360 kPa) and stiff (1000 kPa) microrods, demonstrating the pH-dependent quenching of FITC fluorescence**.**

The FITC/Cy5 ratio was then calculated to normalise for potential variations in fluorophore loading, providing a robust indicator sensitive to environmental pH. All microrod types exhibited a sigmoidal relationship between FITC/Cy5 ratio and pH (Figure 7). It is important to note that the limited number of measured pH values significantly influences this relationship. Ratios remained low and stable at acidic pH values (e.g., pH 4), then increased sharply between pH 6 and 8 before

plateauing under more alkaline conditions. The plateau regions, particularly at highly acidic (e.g., below pH 5) values, represent ranges where the FITC/Cy5 ratio exhibits reduced sensitivity to pH changes[24]. The middle region of the curve (pH 5–7) offers the highest pH resolution, whereas plateau zones (especially below pH 5) limit sensitivity.

These calibration curves provide the essential framework for determining the pH of the intracellular microrods in subsequent experiments.

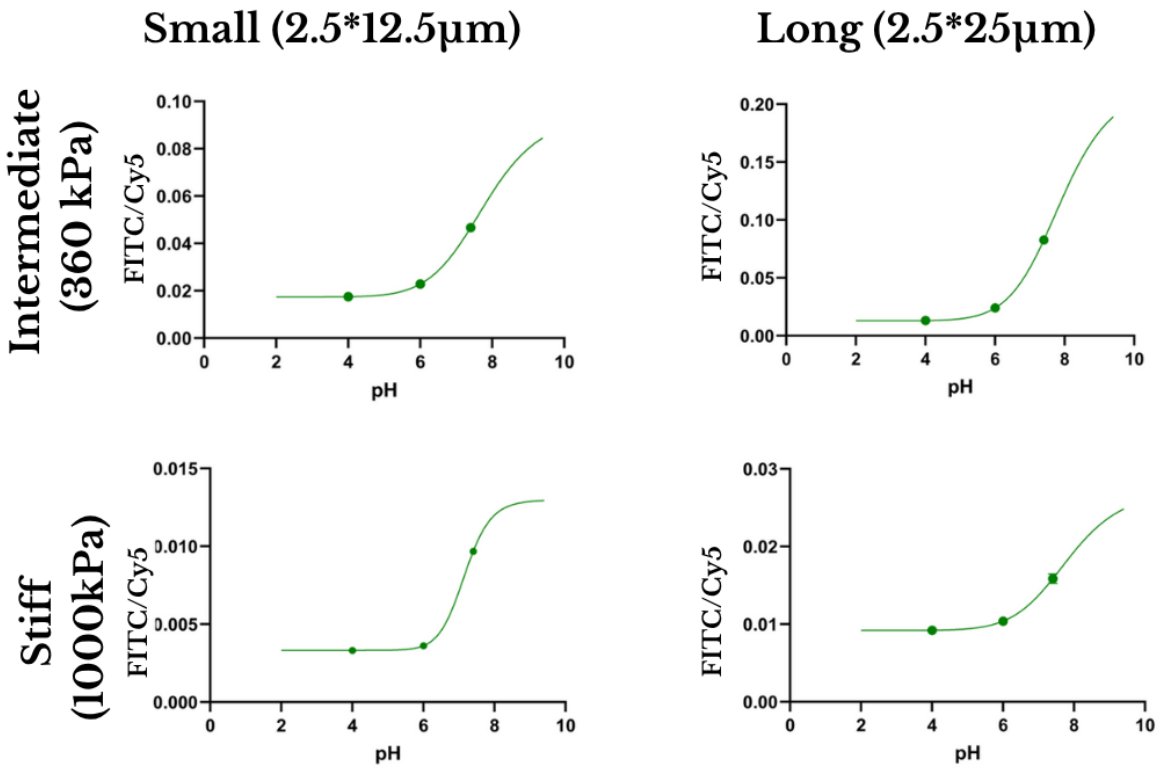

Figure 7: FITC/Cy5 fluorescence ratio as a function of pH for varying microrod sizes and rigidities, modelled with a sigmoidal 4-parameter logistic curve.

Intracellular microrods display varying fluorescence intensities.

Then, we measured intracellular FITC/Cy5 ratios of microrods after 120 min of incubation with J774A.1 macrophage (Figure 8). Gating was used to select cells with a single internalised microrod, to match the conditions from the calibration curves (Supplementary Figure 11). Non-interacting microrods were also measured as controls (Supplementary Figure 12).

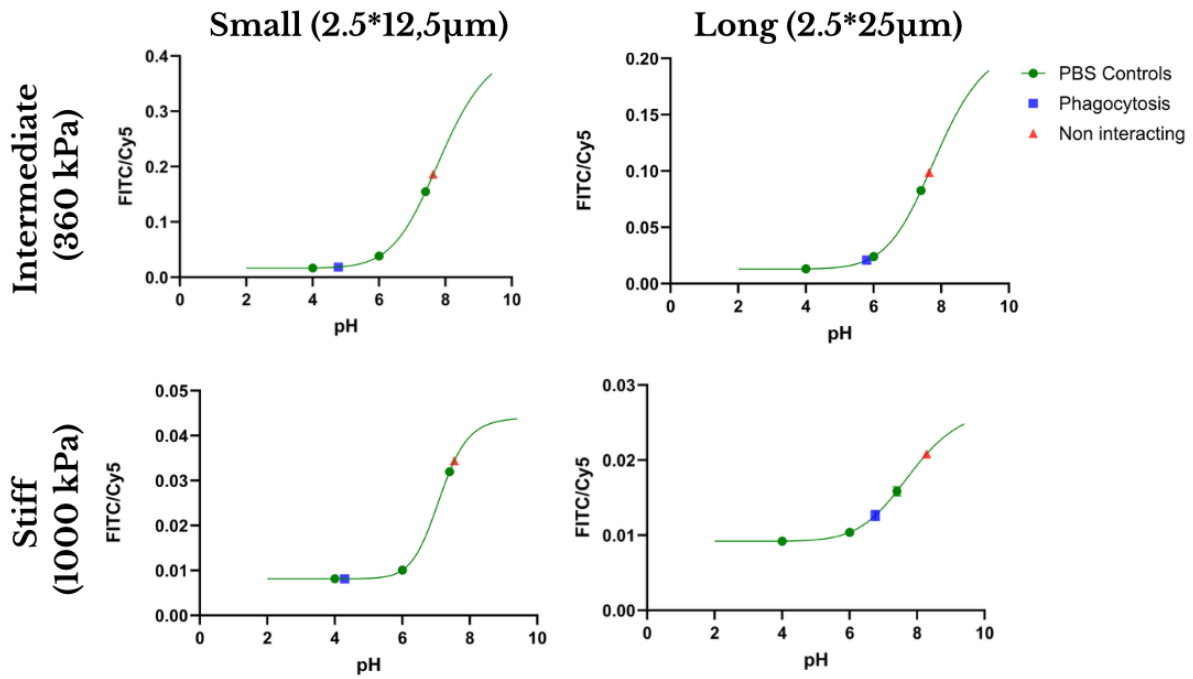

Figure 8: Phagocytosis and non-interacting microrod FITC/Cy5 pH calibration curves for small/long and intermediate/stiff microrods.

As expected, non-interacting microrods exhibited FITC/Cy5 ratios corresponding to pH 7.4, consistent with the physiological pH of the extracellular medium (pH ~ 7.6 for DMEM).

Small microrods (12.5 µm) with both 360 and 1000 kPa stiffness exhibited ratios interpolating to pH 4-6, suggesting that they are efficiently processed through phagosomal maturation. In contrast, long stiff (25 µm; 1000 kPa) microrods remained in a less acidic environment (pH > 6), while intermediate rigidity (360 kPa) showed moderate acidification (pH ~ 6).

To validate cytometry data, we imaged functionalized microrods at pH 4, 6 and 7.4 by fluorescence microscopy. The signal decreased with acidification, matching cytometry results. However, when imaging phagocytosed rods, the FITC signal was outside the calibration range, enabling pH interpolation (Supplementary figure 10). This may be due to signal quenching, photobleaching, or optical distortion within the cell while imaging.

Taken together, these results highlight the interplay between microrod size and rigidity in modulating phagosomal acidification. While small microrods consistently achieved advanced acidification regardless of stiffness, long microrods exhibited a rigidity-dependent acidification profile, where increased stiffness severely impeded the acidification process.

Discussion

In this study, we looked at how the size and stiffness of rod-shaped phagocytic targets affect their uptake and processing by macrophages. We used microrods with different stiffness levels (20, 360, and 1000 kPa) and lengths of 12.5 µm and 25 µm. We discovered that softer rods were always taken up more efficiently than stiffer ones, regardless of their size. Shorter rods also showed

higher uptake across all stiffness levels. By developing a ratiometric FITC/Cy5-based method to measure the intracellular pH of phagocytosed rods, we found that smaller rods, whether soft or stiff, showed a significant drop in pH, which aligns with late-stage phagosomal maturation. In contrast, longer, stiffer rods maintained higher pH levels, indicating poor acidification. Overall, our findings highlight the relationship between size and stiffness in phagosomal processing, where smaller or more flexible rods allow better particle engulfment and acidification, while long, rigid rods experience disrupted maturation.

Rigidity-dependent internalisation is conserved across microrod sizes.

Our flow cytometry-based uptake assays showed that the uptake pattern depended on stiffness and was consistent for both small (12.5 μm) and long (25 μm) rods. Soft 20 kPa rods were taken up more efficiently than stiff 1000 kPa rods. This finding confirms earlier research that indicates soft particles are taken up better because they deform more easily 18,24, reducing the energy needed for membrane wrapping and changes in the cytoskeleton.

Our data underscores that for rod-shaped particles, deformability is a critical factor influencing uptake efficiency, particularly in how it interacts with particle dimensions. This contrasts sharply with results from spherical DAAM particles, where increased stiffness often correlated with enhanced uptake[18], highlighting the unique and increased mechanical challenges that rod-like shapes impose on the phagocytic machinery during engulfment.

One possible explanation for the enhanced uptake of softer rods is that their flexibility permits localised membrane bending and more efficient, partial wrapping around the particle. This likely reduces the overall energy required for membrane protrusion and actin polymerisation during engulfment compared to rigid counterparts. Such localised bending may help the phagocytic cup progress more effectively through the zippering mechanism linked to Fcγ receptor engagement 1,25. While we know that initial receptor engagement can be affected by stiffness [27], our data suggests that this factor plays a minor role in dictating the overall uptake efficiency in this system, particularly given the similar initial interaction rates and early-stage internalisation patterns observed for rods of varying stiffness but the same size. This indicates that the observed differences in overall uptake efficiency are less about the initial contact or binding frequency and more profoundly influenced by the subsequent stages of membrane wrapping and phagocytic cup formation, which are significantly affected by the particle's mechanical flexibility.

On the other hand, stiff rods likely necessitate more extensive and less localised membrane deformation to conform to their shape. This increased energy barrier could disrupt continuous receptor engagement, potentially delaying the engulfment process, prolonging internalisation time, or even leading to premature disassembly of the phagocytic cup. Importantly, our microscopy results (Figure 5) further support this, showing that even stiff rods, particularly smaller ones, were internalised mainly. This suggests that the primary issue for these particles is not a failure of initial internalisation but rather a challenge in subsequent post-internalisation processing, setting up a key distinction that will be explored further in the context of phagosomal maturation. Furthermore, since both small stiff and small soft rods were similarly taken up, this highlights that the key factor is not stiffness alone but how it interacts with particle size, emphasising the significance of flexibility within specific size ranges.

Microscopy reveals shape and stiffness-dependent maturation dynamics.

The observation that stiff, long rods consistently caused actin to accumulate on the ends of the rods suggests that they were unable to progress into the cytoskeletal remodelling phases of phagosome maturation[28]. To further investigate this, we used microscopy to examine actin accumulation following the engulfment of smaller rods. Here, we show that small rods, regardless of rigidity, do not trigger actin accumulation post internalisation. This indicates that the effect of rigidity on actin accumulation is size-dependent.

Interestingly, small rods also did not exhibit bending after internalisation (Figure x). This, combined with our previous observation of bending in longer, softer rods, suggests that bending may play a role in phagosome processing, specifically for larger particles. Indeed, it has been shown that centripetal transport toward the lysosomal compartment is required, as suggested by models of microtubule-based trafficking[27,29]. The accumulation of actin at the ends of stiff, long rods may prevent proper dynein-mediated retrograde transport, resulting in delays in fusion events with the lysosome. In contrast, the smaller size or the bending ability of longer rods may alleviate actin buildup, facilitating the transition from actin to microtubule-based transport and promoting subsequent maturation steps. Future studies can investigate whether stiff rods fail to transition by using live-cell imaging along with cytoskeletal markers, such as phalloidin for actin and EB1 or tubulin-GFP for microtubules. By tracking how actin clears and microtubules move into phagosomes with stiff versus soft rods, it could be possible to see if the mechanical properties affect the cytoskeletal changes needed for maturation [17,22].

pH profiling supports rigidity-dependent maturation defects in large rods

We further show, with the developed ratiometric pH measuring system, that the FITC/Cy5 ratio is a reliable reporter of environmental pH between pH 4 and 7.4. Upon internalisation, small microrods exhibited FITC/Cy5 ratios consistent with acidic pH (4-5), and there was no difference between microrods regardless of stiffness, showing robust phagosomal maturation. Conversely, large 1000 kPa rods had FITC/Cy5 ratios interpolating to pH values >6, indicating a failure to acidify the phagosome. These observations contradict established literature, which shows that large phagosomes acidify more efficiently due to ongoing centripetal trafficking [22]. However, phagosomal remodelling or v-ATPase recruitment may have been interrupted by target stiffness.

From a mechanistic perspective, we hypothesise that rigid rods could block membrane curvature sensing by BAR-domain proteins or phosphoinositide reorganisation, resulting in improper maturation pathways[30]. Another possibility is that the rods' physical rigidity may block efficient recruitment or fusion of lysosomal vesicles by steric hindrance or interference with SNARE complex assembly[14]. The fact that these compartments remain at a higher pH opens the possibility that an acidification defect occurs because of spatially constrained phagosomal membranes that cannot deform sufficiently to fuse with lysosomes.

Limitations and future directions

While our study marks an initial step toward understanding the interplay between target size and stiffness in phagosomal processing, several factors still require further investigation. Here, we investigated phagocytosis via an in vitro system using J774 macrophages. The system lacks in vivo complexity and confounding factors such as opsonisation, macrophage subtype heterogeneity,

and inflammatory signals on phagocytic behaviour. Additionally, FITC/Cy5 ratiometric allowed for efficient pH profiling; however, it had limited resolution at pH < 5, as well as giving no information regarding specific maturation markers like LAMP1 or Rab proteins.

Building upon these limitations, next steps for future studies include tracking live-cell decay of the FITC signal to identify acidification kinetics and examining the recruitment of phagosomal markers, including Rab5 and Rab7, which may inform on the maturation stages that microrod stiffness perturbed (Rab5 for initiation and Rab7 for maturation). The current contributions of mechanical coupling (i.e., cargo geometry, deformation of the membrane, cytoskeleton reorganisation) using force probes and biosensors would enhance or limit the mechanistic capture of the data. Models of mechanical decision-making, combined with experimental disturbance of cytoskeletal regulators, may assess how these mechanical checkpoints constrain immune choices. Additionally, it is yet to be tested whether local force feedback from actin-myosin networks tunes phagosome maturation differentially for deformable versus stiff cargos. We also wonder if there exist mechanical checkpoints during early maturation when insufficient membrane curvature or cytoskeletal tension may interrupt progress toward lysosomal fusion, which can be revisited with live-cell imaging and tension biosensors to understand better the extent to which cargo mechanics regulates the signalling properties of immune cells.

Additionally, it is yet to be tested whether local force feedback from actin-myosin networks tunes phagosome maturation differentially for deformable versus stiff cargos. We wonder if there exist mechanical checkpoints during early maturation when insufficient membrane curvature or cytoskeletal tension may interrupt progress toward lysosomal fusion. This is revisited through live-cell imaging and tension biosensors to understand better how cargo mechanics regulates the signalling properties of immune cells.

Together, our findings collectively support a model whereby target geometry and rigidity significantly regulate phagocytic progression. While stiff spherical particles may be taken up more efficiently [18], our data demonstrates that elongate shapes, such as microrods, appear to necessitate deformability for successful internalisation and subsequent maturation. Overall, our results further support the growing understanding that phagocytic mechanosensing involves a crucial linkage between cytoskeletal tension and cargo deformation [2,18]. Our research contributes explicitly to this understanding by revealing how the interplay of particle size and stiffness dictates not only initial uptake efficiency but also critically influences downstream phagosomal processing, especially for larger, non-spherical constructs. This emphasises the complex mechanical dialogue occurring at the host-pathogen interface and provides a foundation for designing biomaterials with tailored immune responses.

Bibliography

1. Vorselen, D. *et al.* Phagocytic 'teeth' and myosin-II 'jaw' power target constriction during phagocytosis. *Elife* **10**, (2021).

2. Vorselen, D., Labitigan, R. L. D. & Theriot, J. A. A mechanical perspective on phagocytic cup formation. *Current Opinion in Cell Biology* vol. 66 112–122 Preprint at https://doi.org/10.1016/j.ceb.2020.05.011 (2020).

3. Vorselen, D. *et al.* Microparticle traction force microscopy reveals subcellular force exertion patterns in immune cell–target interactions. *Nat Commun* **11**, 20 (2020).

4. Schuermans, S., Kestens, C. & Marques, P. E. Systemic mechanisms of necrotic cell debris clearance. *Cell Death & Disease 2024 15:8* **15**, 1–16 (2024).

5. Sly, L. M. & McKay, D. M. Macrophage immunotherapy: overcoming impediments to realize promise. *Trends Immunol* **43**, 959–968 (2022).

6. Mantovani, A., Allavena, P., Marchesi, F. & Garlanda, C. Macrophages as tools and targets in cancer therapy. *Nat Rev Drug Discov* **21**, 799–820 (2022).

7. Klichinsky, M. *et al.* Human chimeric antigen receptor macrophages for cancer immunotherapy. *Nat Biotechnol* **38**, 947–953 (2020).

8. Wang, L. *et al.* Promoting macrophage phagocytosis of cancer cells for effective cancer immunotherapy. *Biochem Pharmacol* **232**, (2025).

9. Murray, P. J. & Wynn, T. A. Protective and pathogenic functions of macrophage subsets. *Nat Rev Immunol* **11**, 723–737 (2011).

10. Brown, G. C. Cell death by phagocytosis. *Nat Rev Immunol* **24**, 91–102 (2024).

11. Omer, S., Li, J., Yang, C. X. & Harrison, R. E. Ninein promotes F-actin cup formation and inward phagosome movement during phagocytosis in macrophages. *Mol Biol Cell* **35**, ar26 (2024).

12. Coppolino, M. G. *et al.* Evidence for a molecular complex consisting of Fyb/SLAP, SLP-76, Nck, VASP and WASP that links the actin cytoskeleton to Fcγ receptor signalling during phagocytosis. *J Cell Sci* **114**, 4307–4318 (2001).

13. Yu, Y., Zhang, Z. & Yu, Y. Timing of Phagosome Maturation Depends on Their Transport Switching from Actin to Microtubule Tracks. *J Phys Chem B* **127**, 9312–9322 (2023).

14. Pauwels, A. M., Trost, M., Beyaert, R. & Hoffmann, E. Patterns, Receptors, and Signals: Regulation of Phagosome Maturation. *Trends Immunol* **38**, 407–422 (2017).

15. Vieira, O. V., Botelho, R. J. & Grinstein, S. Phagosome maturation: aging gracefully. *Biochemical Journal* **366**, 689–704 (2002).

16. Fairn, G. D. & Grinstein, S. How nascent phagosomes mature to become phagolysosomes. *Trends Immunol* **33 8**, 397–405 (2012).

17. Nguyen, J. A. & Yates, R. M. Better Together: Current Insights Into Phagosome-Lysosome Fusion. *Frontiers in Immunology* vol. 12 Preprint at https://doi.org/10.3389/fimmu.2021.636078 (2021).

18. Baranov, M. V., Kumar, M., Sacanna, S., Thutupalli, S. & van den Bogaart, G. Modulation of Immune Responses by Particle Size and Shape. *Frontiers in Immunology* vol. 11 Preprint at https://doi.org/10.3389/fimmu.2020.607945 (2021).

19. Méresse, S. *et al.* Remodelling of the actin cytoskeleton is essential for replication of intravacuolar Salmonella. *Cell Microbiol* **3**, 567–577 (2001).

20. Naj, X. & Linder, S. ER-Coordinated Activities of Rab22a and Rab5a Drive Phagosomal Compaction and Intracellular Processing of Borrelia burgdorferi by Macrophages. *Cell Rep* **12**, 1816–1830 (2015).

21. Beningo, K. A. & Wang, Y. L. Fc-receptor-mediated phagocytosis is regulated by mechanical properties of the target. *J Cell Sci* **115**, 849–856 (2002).

22. Keller, S., Berghoff, K. & Kress, H. Phagosomal transport depends strongly on phagosome size. *Sci Rep* **7**, (2017).

23. Boesveld, S. *et al.* Microgels as Platforms for Antibody-Mediated Cytokine Scavenging. *Adv Healthc Mater* **12**, 2300695 (2023).

24. Ohgaki, R. *et al.* Ratiometric fluorescence imaging of cell surface pH by poly(ethylene glycol)-phospholipid conjugated with fluorescein isothiocyanate. *Sci Rep* **7**, 17484 (2017).

25. Richards, D. M. & Endres, R. G. Target shape dependence in a simple model of receptor-mediated endocytosis and phagocytosis. *Proceedings of the National Academy of Sciences* **113**, 6113–6118 (2016).

26. Jaumouillé, V. & Waterman, C. M. Physical Constraints and Forces Involved in Phagocytosis. *Frontiers in Immunology* vol. 11 Preprint at https://doi.org/10.3389/fimmu.2020.01097 (2020).

27. Araki, N. Role of microtubules and myosins in Fc gamma receptor-mediated phagocytosis. *Frontiers in Bioscience* **11**, 1479 (2006).

28. Settle, A. H. *et al.* β 2 integrins impose a mechanical checkpoint on macrophage phagocytosis. Preprint at https://doi.org/10.1101/2024.02.20.580845 (2024).

29. Harrison, R. E. & Grinstein, S. Phagocytosis and the microtubule cytoskeleton. *Biochemistry and Cell Biology* **80**, 509–515 (2002).

30. Carman, P. J. & Dominguez, R. BAR domain proteins—a linkage between cellular membranes, signaling pathways, and the actin cytoskeleton. *Biophys Rev* **10**, 1587–1604 (2018).

Appendix

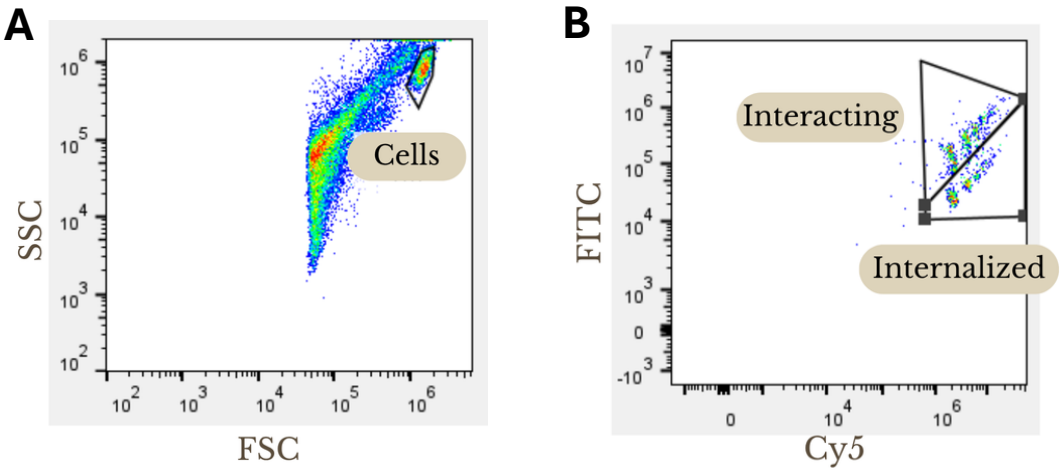

Figure 9: The analysis extracted from the flow cytometer after the phagocytic assay. The functionalized microrods. A represents the forward (FSC) vs side scatter (SSC), using which the cells are gated. Following that, based on FITC quenching, interacting and internal microrods were visualised (B).

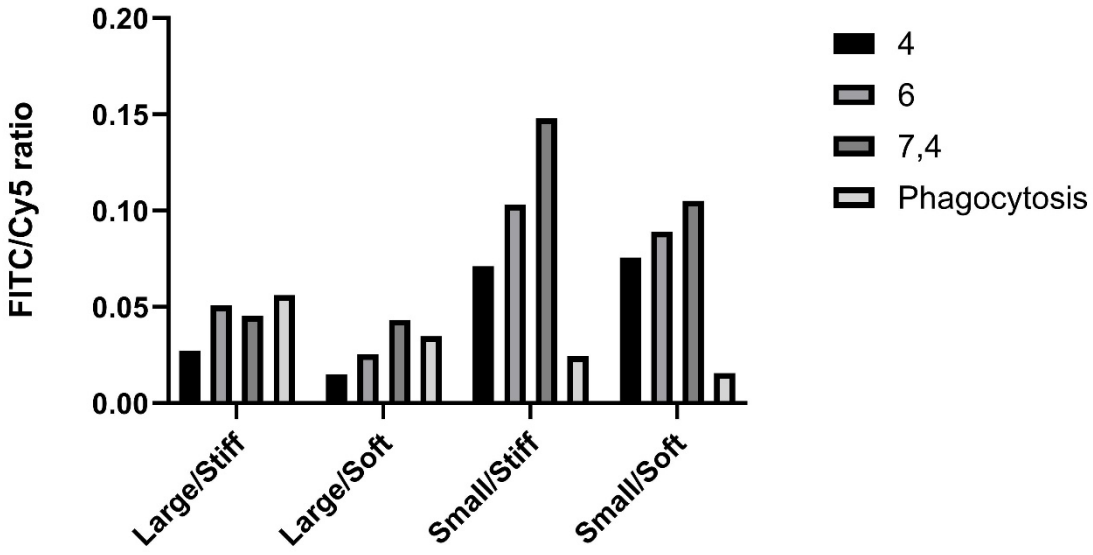

Figure 10: Microscopy Phagocytosis microrod FITC/Cy5 ratios and pH calibration measures for small/long and intermediate/stiff microrods

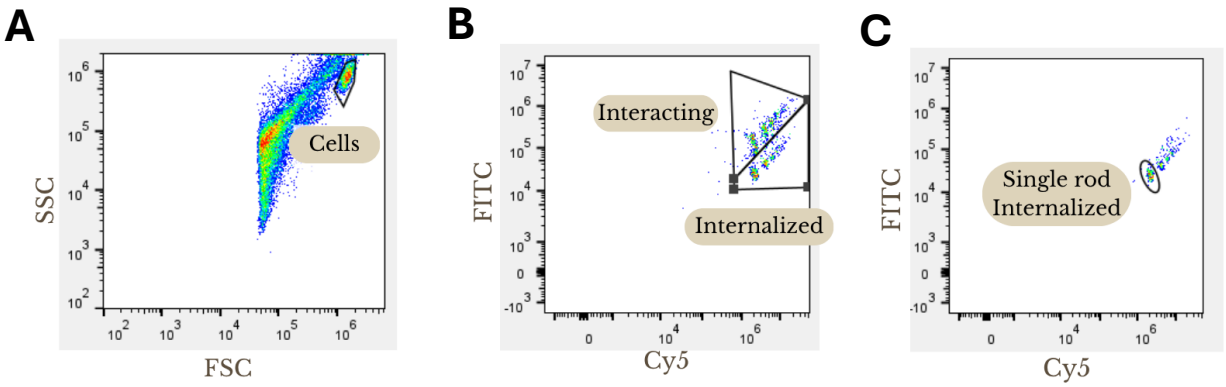

*Figure 11: The analysis extracted from the flow cytometer after phagocytic assay with the functionalized microrods. **A** represents the forward (FSC) vs side scatter (SSC) used to gate the cells. Following that, based on FITC quenching, interacting and internal microrods were visualised (B). Then, based on Cy5 quenching, cells that have internalised a single rod were further analysed (C).*

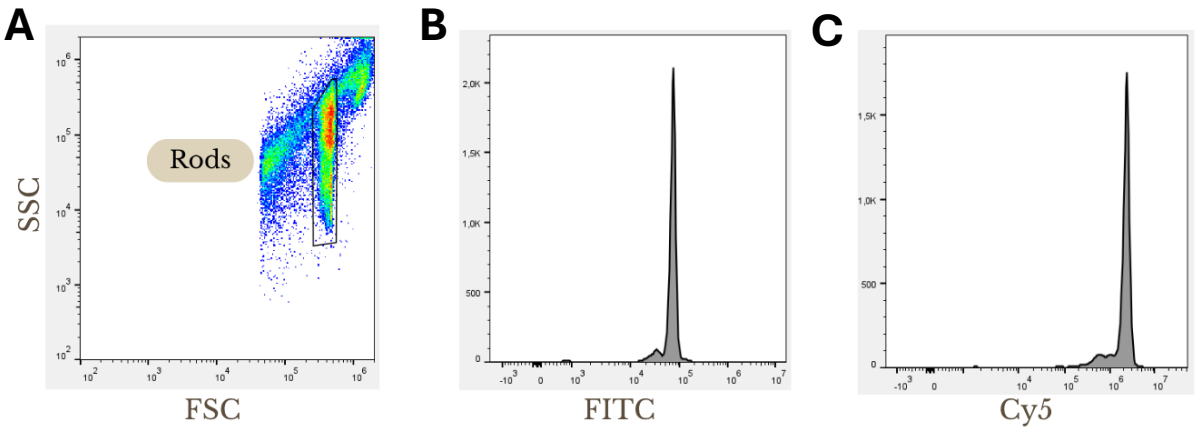

*Figure 12: The analysis extracted from the flow cytometer after phagocytic assay with the functionalized microrods. **A** represents the forward (FSC) vs side scatter (SSC) used to gate the rods. FITC and Cy5 histograms were subsequently obtained (B and C).*